

# Interaction of GRB fireballs with ambient medium

*Andrei M. Beloborodov*  
*Canadian Institute for Theoretical Astrophysics*  
*University of Toronto, 60 St. George Street*  
*Toronto, M5S 3H8 Ontario, CANADA*

## Abstract

The customary picture of the fireball deceleration by an external medium neglects two physical agents in the problem that are important at radii  $R < 10^{17}$  cm: a radiative precursor (the prompt GRB) and a relativistic front of free neutrons. The radiative precursor preaccelerates the medium and loads it with  $e^\pm$  pairs. This provides a new explanation for the early optical flashes in GRBs. The front of free neutrons must form in a standard baryonic fireball and change the mechanism of the fireball deceleration. The neutron effect, however, disappears if the fireball is strongly dominated by the Poynting flux. The neutrons thus provide a unique link between the progenitor physics and the observed external blast wave. The explosion mechanism at  $R < 10^{17}$  cm is testable with upcoming observations of early afterglows.

## 1 Introduction

The picture of an ultra-relativistic shell (“fireball”) ejected by a central engine became a customary model of GRBs. The shell emits the burst of  $\gamma$ -rays, sweeps up a static ambient medium, and decelerates, producing the afterglow emission. This simple model is consistent with the observational data. Recently, however, it has been realized to be intrinsically inconsistent at radii up to  $R \sim 10^{17}$  cm. The picture is missing two physical agents that appear inevitably in the model:

(1) The prompt burst of  $\gamma$ -rays acts as a powerful precursor ahead of the fireball. It dramatically changes the early phase explosion, at radii  $R < 2 \times 10^{16} E_{53}^{1/2}$  cm where  $E$  [erg] is the isotropic energy equivalent of the  $\gamma$ -ray burst.

(2) The standard GRB fireball contains free neutrons. An interesting fraction of neutrons survive up to  $R \approx 8 \times 10^{16} (\Gamma_{\text{ej}}/300)$  cm and changes the mechanism of the fireball-medium interaction.

Here, we describe these advances in the fireball physics. The radiative precursor turns out to have an important connection with the prompt optical flashes observed in GRBs — it offers a new explanation for the flash, alternative to the reverse-shock

interpretation; this explanation works for the Poynting-dominated as well as barynic fireballs.

## 2 Radiative precursor

Radiative precursors are known to be important for interstellar shocks [1]. In the case of GRB explosion, there is an evident fierce precursor: the initial burst of  $\gamma$ -rays with the isotropic energy equivalent up to  $3 \times 10^{54}$  erg. The  $\gamma$ -rays come to the observer before the afterglow,<sup>1</sup> so they must propagate ahead of the blast wave and impact the external medium. This loophole of the GRB model has been noted recently [2]-[5]. Two major effects of the  $\gamma$ -ray precursor are preacceleration of the ambient medium and its loading with  $e^\pm$  pairs. The exact numerical calculation of the medium dynamics in the precursor has been done and understood analytically [5]. It is summarized and explained below.

Let  $dE/dS$  be the energy column density of the  $\gamma$ -ray front [erg/cm<sup>2</sup>]. The GRB is likely beamed, yet it is convenient to define its isotropic equivalent  $E = 4\pi R^2(dE/dS)$ . When an ambient electron is overtaken by the radiation front, it scatters energy  $e_{sc} = \sigma_T(dE/dS) = E\sigma_T/4\pi R^2$  (with a slight modification due to Klein-Nishina correction to Thomson cross section  $\sigma_T$ ). The  $e_{sc}$  should be compared with the electron rest-mass energy, and this gives the relevant dimensionless parameter,

$$\xi = \frac{e_{sc}}{m_e c^2} = 65 E_{53} R_{16}^{-2}. \quad (1)$$

One would like to know the velocity  $\beta$  acquired by the medium behind the radiation front and the number of loaded pairs per one ambient electron,  $f = n_\pm/n_e$ . The medium dynamics in the front is nonlinear because the scattered photons turn into  $e^\pm$  pairs which do more scattering, and the problem is further complicated by the transfer of the scattered radiation across the front. Yet an exact solution can be obtained and well approximated by a simple analytical model [5],

$$\gamma(\xi) = \begin{cases} 1 & \xi < \xi_{acc}, \\ (\xi/\xi_{acc})^3 & \xi_{acc} < \xi < 3\xi_{acc}, \\ 3\sqrt{3}(\xi/\xi_{acc})^{3/2} & \xi > 3\xi_{acc}, \end{cases} \quad (2)$$

$$f(\xi) = \begin{cases} \frac{1}{2}[\exp(\xi/\xi_{load}) + \exp(-\xi/\xi_{load})] & \xi < \xi_{acc}, \\ (\xi/\xi_{acc})^2 f_{acc} & \xi_{acc} < \xi < 3\xi_{acc}, \\ 3(\xi/\xi_{acc}) f_{acc} & \xi > 3\xi_{acc}, \end{cases} \quad (3)$$

---

<sup>1</sup>In fact, the  $\gamma$ -rays can be emitted quite early inside the fireball, preceding the development of the external blast wave. The strong ms variability in GRB light curves is often cited as an evidence for small radius of  $\gamma$ -ray emission  $R \sim 10^{12} - 10^{14}$  cm; the ensuing blast wave radiates at  $R \sim 10^{15} - 10^{17}$  cm.

where  $\xi_{\text{load}} = 20 - 30$ , depending on the spectrum of the gamma-rays,  $\xi_{\text{acc}} = 5\xi_{\text{load}} = 100 - 150$ , and  $f_{\text{acc}} = [\exp(\xi_{\text{acc}}/\xi_{\text{load}}) + \exp(-\xi_{\text{acc}}/\xi_{\text{load}})]/2 = 74$ .

If  $\xi < \xi_{\text{load}}$  nothing interesting happens with the medium in the  $\gamma$ -ray front: it remains almost static and  $e^\pm$ -free. If the front has  $\xi > \xi_{\text{load}}$ , the runaway  $e^\pm$  loading occurs. The number of loaded pairs depends exponentially on  $\xi$  as long as  $\xi < \xi_{\text{acc}}$ . The front acts as a relativistic accelerator if  $\xi > \xi_{\text{acc}}$ , and the medium Lorentz factor  $\gamma$  grows with  $\xi$  as a power-law. At  $\xi = \xi_{\text{gap}} \approx 3 \times 10^3$ ,  $\gamma$  exceeds the Lorentz factor of the ejecta; it implies that the radiative precursor pushes the external medium away from the fireball and opens a gap.

The  $\gamma$ -ray front expands with time, and its  $\xi$ -parameter evolves as  $\xi \propto R^{-2}$  (Eq. 1), i.e., decreases. It starts at very high  $\xi$  and then passes through  $\xi_{\text{gap}}$ ,  $\xi_{\text{acc}}$ , and  $\xi_{\text{load}}$  at radii  $R_{\text{gap}}$ ,  $R_{\text{acc}}$ , and  $R_{\text{load}}$ , respectively,

$$R_{\text{acc}} \approx 10^{16} E_{53}^{1/2} \text{ cm}, \quad R_{\text{gap}} \approx R_{\text{acc}}/3, \quad R_{\text{load}} = 2.3R_{\text{acc}}. \quad (4)$$

The three characteristic radii define four stages of the explosion:

**I.**  $R < R_{\text{gap}}$ . The ejecta move in a cavity cleared by the radiation front. The ambient medium surfs ahead with  $\gamma > \Gamma_{\text{ej}}$ .

**II.**  $R_{\text{gap}} < R < R_{\text{acc}}$ . The ejecta sweep the  $e^\pm$ -rich medium that has been preaccelerated to  $1 \ll \gamma < \Gamma_{\text{ej}}$ .

**III.**  $R_{\text{acc}} < R < R_{\text{load}}$ . The ejecta sweep the practically static medium ( $\gamma \approx 1$ ). The medium is, however, dominated by the loaded  $e^\pm$ .

**IV.**  $R > R_{\text{load}}$ . The ejecta sweep the static pair-free medium. The precursor effect is negligible.

The blast wave develops at  $R > R_{\text{gap}}$ . Technically, its model is constructed in the same way as it was done for a static external medium. The only complication is that now the preshock material is  $e^\pm$ -rich and moving relativistically. At  $R = R_{\text{gap}}$  the blast wave gently begins to sweep up the preaccelerated medium with a small relative Lorentz factor,  $\Gamma_{\text{rel}} \approx \Gamma_{\text{ej}}/\gamma \approx 1$ . With increasing  $R > R_{\text{gap}}$ ,  $\gamma$  falls off quickly and approaches  $\gamma = 1$  at  $R = R_{\text{acc}}$  as  $\gamma = (R/R_{\text{acc}})^{-6}$ . Thus, the fireball suddenly “learns” that there is an interesting amount of relatively slow material on its way and hits it with a large  $\Gamma_{\text{rel}}$ . This resembles a collision with a wall and results in a sharp rise in dissipation at  $R \approx R_{\text{acc}}$  (see Fig. 4 in [5]). This dynamic effect is especially dramatic for GRBs with massive progenitors. Their ambient medium is a dense wind from the progenitor and the swept-up mass at  $R_{\text{acc}}$ ,  $m_{\text{acc}} = m(R_{\text{acc}})$ , (the “wall”) can exceed  $E_{\text{ej}}/\Gamma_{\text{ej}}^2 c^2$ , where  $E_{\text{ej}}$  is the total fireball energy. Then the delayed collision with  $m_{\text{acc}}$  is the main dissipation event in the history of the explosion.

We note here that the optically thin medium scatters only a small portion of the  $\gamma$ -ray energy. In view of this fact, the strong dynamical impact of the  $\gamma$ -ray precursor on the fireball deceleration might seem surprising. The clue to this paradox is the high Lorentz factor of the fireball,  $\Gamma_{\text{ej}} \gg 1$ . Because of high  $\Gamma_{\text{ej}}$ , a small ambient mass

is expected to efficiently decelerate the fireball: half of  $E_{\text{ej}}$  would be dissipated when the fireball sweeps up a static  $m = E_{\text{ej}}/\Gamma_{\text{ej}}^2 c^2$  [6]. If, however, the fireball sends ahead a radiation precursor, it easily preaccelerates the medium to  $\gamma \gg 1$  by depositing a relatively small energy  $\gamma mc^2 \ll E_{\text{ej}}$ . Even at  $\gamma > \Gamma_{\text{ej}}$ , the deposited energy is small, while the dynamical impact is enormous:  $m$  runs away and the fireball moves freely in the cavity cleared by the  $\gamma$ -ray precursor. Thus, the fireball dissipation is delayed until the precursor is diluted sufficiently by side expansion.

The described scenario is modified if the  $\gamma$ -ray front is created by the blast wave itself rather than by internal dissipation in the fireball. Then a self-consistent blast wave model can be obtained without gap opening. If, however, the ambient medium is sufficiently dense then an “electro-magnetic catastrophe” can occur in the forward shock as described in [7]. The runaway production of  $\gamma$ -rays may result in a temporary gap opening and complicated temporal evolution of the shock. The feedback of the  $\gamma$ -ray precursor on the shock is a major agent governing this evolution.

### 3 The prompt optical flash

The optical flash was first detected in GRB 990123 [8]. It occurs much earlier than the normal optical afterglow that is observed days after the  $\gamma$ -ray burst. In GRB 990123, the optical flash peaked less than minute after the GRB trigger. It was explained (and in fact predicted) as a possible emission from the reverse shock in the ejecta [9, 10]. This explanation would exclude the Poynting-flux models of GRB ejecta where the reverse shock is energetically unimportant or does not occur at all. This explanation, however, is not unique.

In fact, even in the absence of any emission from the reverse shock, one expects a soft flash from the *forward* shock [5]. The blast wave evolution described above implies that the afterglow starts with a brief and very soft flash. It results from the pair loading and preacceleration of the ambient medium by the  $\gamma$ -ray front.

One can evaluate the effect using the customary synchrotron emission model. In the blast frame, the synchrotron spectrum of  $e^\pm$  with Lorentz factor  $\gamma_e$  peaks at

$$\tilde{\nu}_s = 10^6 B \gamma_e^2 \text{ Hz}, \quad (5)$$

where  $B$  is the postshock magnetic field. The observed peak frequency is  $\nu_s \approx \Gamma \tilde{\nu}_s$ , where  $\Gamma$  is the current Lorentz factor of the blast.  $B$  is usually parametrized in terms of the equipartition value, so that  $B^2/8\pi$  is a fraction  $\epsilon_B$  of the total energy density. Using the jump conditions at the shock front, one can write

$$B = c \frac{\Gamma}{\gamma} \sqrt{\frac{32\pi\epsilon_B\rho_0}{\gamma(1-\beta)}}. \quad (6)$$

Thus, preacceleration of the preshock medium to  $\gamma > 1$  reduces  $B$  by a factor of  $\gamma^{-1/2}$ .

A fraction  $\epsilon_e \sim 0.01 - 0.1$  of the energy of shocked ions is shared by  $e^\pm$ . The mean randomized Lorentz factor of the postshock  $e^\pm$  is

$$\gamma_e \approx \frac{\Gamma}{\gamma} \frac{m_p}{f m_e} \epsilon_e, \quad (7)$$

where  $f = n_\pm/n_e$  is the pair loading factor. Substituting Eqs. (6) and (7) into (5), one finds that the  $\gamma$ -ray precursor reduces the synchrotron peak frequency  $\nu_s$  by the factor of  $\gamma^{-5/2} f^{-2}$ . This is a big effect at all  $R < R_{\text{load}} \approx 2 \times 10^{16} E_{53}^{1/2}$  cm. The afterglow should start as a very soft signal, and it quickly hardens as  $\gamma(R)$  and  $f(R)$  decrease steeply with radius [see Eqs. (1-3)]. A maximum  $\nu_s$  is achieved at  $R_{\text{acc}} \lesssim R \lesssim R_{\text{load}}$ , and then the usual decay sets in (see also Fig. 6 in [5]).

The initial soft flash should have a broad spectrum and can be observed in the optical band. It appears to be an inevitable result of the preacceleration and  $e^\pm$ -loading of the ambient medium. Because the flash is emitted by the forward shock, this mechanism works regardless the nature of the GRB ejecta. It applies to Poynting-flux ejecta as well as to standard baryonic fireballs.

One can easily evaluate the arrival time of the expected flash. The flash should peak at observed time

$$t_{\text{flash}} \approx \frac{R_{\text{acc}}}{2\Gamma_{\text{ej}}^2} (1+z) \approx 12 E_{53}^{1/2} \left( \frac{\Gamma_{\text{ej}}}{100} \right)^{-2} \left( \frac{1+z}{3} \right) \text{ s}, \quad (8)$$

where  $z$  is the cosmological redshift of the burst. A nice feature of this prediction is that  $t_{\text{flash}}$  depends only on the isotropic equivalent of the burst energy,  $E$ , and the initial Lorentz factor of the ejecta,  $\Gamma_{\text{ej}}$ . If one manages to observe the peak of the flash and measure the burst redshift (which gives  $E$ ), then one can infer  $\Gamma_{\text{ej}}$  — the unknown and probably most important parameter of the GRB phenomenon. The optical flash in GRB 990123 peaked at  $t_{\text{flash}} \approx 20$  s (corrected for cosmological time dilation) and the isotropic  $\gamma$ -ray energy of the burst was  $E \approx 3 \times 10^{54}$  erg [7]. Eq. (8) then implies  $\Gamma_{\text{ej}} \approx 200$ . This result does not depend on  $\epsilon_B$ ,  $\epsilon_e$ ,  $n_0$ , the beaming angle and the nature of the ejecta, or any other parameters of the explosion.

The energy of the pair-loaded flash is approximately

$$E_{\text{flash}} \sim m_{\text{acc}} c^2 \Gamma^2, \quad (9)$$

where  $m_{\text{acc}}$  is the ambient mass within  $R_{\text{acc}}$ . If  $m_{\text{acc}} < E_{\text{ej}}/\Gamma_{\text{ej}}^2 c^2$  (i.e.  $R_{\text{acc}}$  is smaller than the characteristic deceleration radius of the fireball  $R_{\text{dec}}$ ) then  $\Gamma \approx \Gamma_{\text{ej}}$  during the flash; the main peak of the afterglow occurs later at  $R = R_{\text{dec}}$  and emits more energy (in the X-ray bands). Then  $E_{\text{flash}}$  is a small fraction of the total energy of the explosion. In the case of a homogeneous ambient medium with density  $n_0 = \text{const}$ , one finds [5]

$$\frac{E_{\text{flash}}}{E_{\text{ej}}} \approx 10^{-3} n_0 \left( \frac{\Gamma_{\text{ej}}}{300} \right)^2 \frac{E_{53}^{3/2}}{E_{\text{ej}53}}. \quad (10)$$

GRBs with massive progenitors occur inside dense star-forming clouds with  $n_0 \sim 1-10^2 \text{ cm}^{-3}$  and a detectable flash is expected. Even more importantly, the progenitor itself emits a powerful wind all the time before it explodes, and its wind is the actual ambient medium of the GRB (with density scaling with radius as  $R^{-2}$  out to a parsec distance). The wind from a Wolf-Rayet progenitor can easily have  $m_{\text{acc}} > E_{\text{ej}}/\Gamma_{\text{ej}}^2 c^2$ . Then the main fireball dissipation occurs at  $R \sim R_{\text{acc}}$  in the medium heavily loaded with  $e^\pm$ ; the resulting powerful soft flash coincides with the main peak of the afterglow [5].

By now the early optical emission has been detected in four bursts: GRB 990123, GRB 021004, GRB 021211, and GRB 030329. The initial peak of the optical emission has been seen only in GRB 990123. This is naturally explained by the model described above: the flash should peak earlier than 10 s unless  $\Gamma_{\text{ej}} < 100 E_{53}^{1/2} (1+z)^{1/2}$  (see Eq. 8), and therefore it is difficult to detect the peak with current instruments. The proposed microsatellite *ECLAIRs* [11] would be very helpful as it can provide data in soft bands at all times, even much shorter than 10 s.

## 4 Neutron front

An intriguing aspect of the GRB explosion, again related to the ultra-relativistic character of the explosion, is a significant contamination of the fireball by free neutrons [12]-[18]. Besides opening a possibility to observe multi-GeV neutrinos generated by neutron-ion collisions, it has important implications for the afterglow physics: the very mechanism of the afterglow can be changed by neutrons at radii up to  $10^{17} \text{ cm}$  [19].

### 4.1 Neutronization of the Central Engine

What is ejected in a GRB explosion? Its engine is very dense and hot, and the central matter (or the matter surrounding the central black hole) is filled with  $e^\pm$  pairs in thermodynamic equilibrium with blackbody radiation at a temperature  $kT = 1-10 \text{ MeV}$ . Its baryonic component is made of neutrons and protons (composite nuclei break up into free nucleons in the unshadowed region of the  $T - \rho$  plane in Fig. 1) and frequent  $e^\pm$  captures onto nucleons take place,

$$e^- + p \rightarrow n + \nu, \quad e^+ + n \rightarrow p + \bar{\nu}. \quad (11)$$

These reactions quickly convert protons to neutrons and back, and establish an equilibrium proton fraction  $Y_e = n_p/(n_n + n_p)$  which is shown in Figure 1. Any plausible GRB engines belong to the  $T - \rho$  region where  $Y_e < 0.5$  (see [18] and refs. therein). So, the neutrons are not only present in the central engines — they dominate.

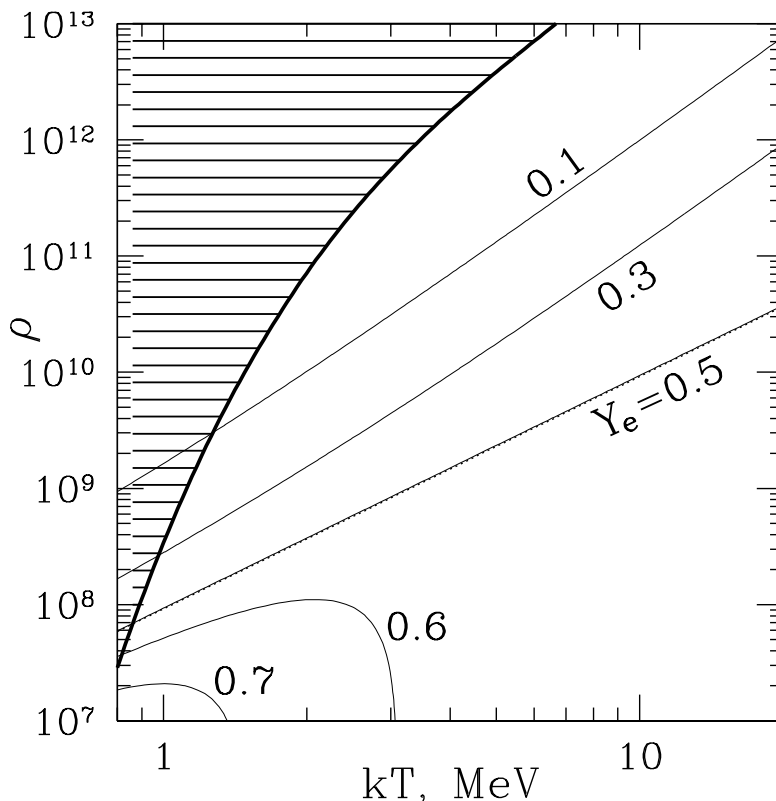


Figure 1: Contours of equilibrium  $Y_e = n_p/(n_n+n_p)$  on the  $T$ - $\rho$  plane for  $\nu$ -transparent matter. Thick curve shows the boundary of free-nucleon region. A similar plot for  $\nu$ -opaque matter is shown in [18].

When the neutronized matter is ejected into a high-entropy fireball, it remains neutron-dominated because (1) expansion occurs too fast and  $Y_e$  freezes out at its initial value below 0.5, or (2) the fireball partially absorbs the neutrino flux from the engine, which tends to keep  $Y_e < 0.5$  (see [18] for details).

## 4.2 Ejected Neutrons Survive the Nucleosynthesis

As the fireball expands and cools, free nucleons tend to recombine into  $\alpha$ -particles (like they do in the big bang). This process competes, however, with rapid expansion and can freeze out. For this reason, nucleosynthesis is suppressed in fireballs with a high photon-to-baryon ratio  $\phi = n_\gamma/n_b$  (or, equivalently, high entropy per baryon  $s/k = 3.6\phi$ ). A minimum  $\phi$  in GRBs is  $\sim 10^5$ , which is just marginal for nucleosynthesis (detailed nucleosynthesis calculations have been done recently in [18],[20],[17]). Even in the extreme case of complete helium production, however, there are still leftover

neutrons because of the neutron excess ( $Y_e < 0.5$ ). The nucleon recombination into  $\alpha$ -particles consumes equal numbers of  $p$  and  $n$ , and the minimum mass fraction of leftover neutrons is  $X_n = 1 - 2Y_e$ .<sup>2</sup>

In addition, the synthesized helium is likely destroyed during the ensuing evolution of the explosion [18]. This happens if (1) there appears a significant relative bulk velocity between the neutron and ion components (as a result of neutron decoupling during the acceleration stage of the fireball) or (2) internal shocks occur and heat the ions to a high temperature.

Thus, a substantial neutron component appears inevitably in the standard fireball scenario. The neutrons develop a Lorentz factor  $\Gamma_n = 10^2 - 10^3$  at the very beginning of the explosion when the fireball is accelerated by radiation pressure; they are collisionally coupled to the ions in the early dense fireball, and decouple close to the end of the acceleration stage. Then the neutrons coast and gradually decay with a mean lifetime  $\tau_\beta \approx 900$  s and a mean decay radius  $R_\beta = c\tau_\beta\Gamma_n$ ,

$$R_\beta = 0.8 \times 10^{16} \left( \frac{\Gamma_n}{300} \right) \text{ cm.} \quad (12)$$

We will show below that neutrons change the fireball-medium interaction at radii as large as  $10R_\beta$ .

### 4.3 Neutron-Fed Blast Wave

Let us remind what happens in a relativistic explosion without neutrons. The ejected fireball with mass  $M_{\text{ej}} = E_{\text{ej}}/\Gamma_{\text{ej}}c^2$  and Lorentz factor  $\Gamma_{\text{ej}}$  sweeps up an ambient medium with density  $n_0 = 1 - 10^2 \text{ cm}^{-3}$  and gradually dissipates its kinetic energy. The dissipation rate peaks at a characteristic “deceleration” radius  $R_{\text{dec}} \sim 10^{16} \text{ cm}$  where half of the initial energy is dissipated.  $R_{\text{dec}}$  corresponds to swept-up mass  $m_{\text{dec}} = M_{\text{ej}}/\Gamma_{\text{ej}}$ . Further dynamics is described by the self-similar blast wave model. How does this picture change in the presence of neutrons?

At radii under consideration,  $R > 10^{15} \text{ cm}$ , the ejected fireball is a shell of thickness  $\Delta \ll R$ . In contrast to neutrons, the ion component of the fireball is aware of the external medium and its Lorentz factor  $\Gamma$  decreases. As  $\Gamma$  decreases below  $\Gamma_n$ , the ions fall behind and separate from the neutrons. Thus the fireball splits into two relativistic shells which we name N (neutrons) and I (ions). The mass of the leading N-shell is decreasing because of the  $\beta$ -decay,

$$M_n(R) = M_n^0 \exp\left(-\frac{R}{R_\beta}\right). \quad (13)$$

---

<sup>2</sup>For a similar reason, 75% of baryons in the universe are protons. There was a proton excess at the time of primordial nucleosynthesis with  $Y_e \approx 7/8$ . After nucleon recombination, it resulted in mass fraction  $X_p = 2Y_e - 1 = 0.75$  of leftover protons.

The N-shell energy,  $E_n = \Gamma_n M_n c^2$ , remains, however, huge compared to the ambient rest-mass  $mc^2$  even at  $R > R_\beta$ . For example, at  $R = R_{\text{dec}}$  one finds  $E_n/m_{\text{dec}}c^2 = X_n \Gamma_n \Gamma_{\text{ej}} \exp(-R_{\text{dec}}/R_\beta)$  where  $X_n = M_n^0/M_{\text{ej}}$  is the initial neutron fraction of the fireball.

The neutron decay products  $p$  and  $e^-$  share immediately their huge momentum with ambient particles due to two-stream instability and the N-shell leaves behind a mixed trail with a relativistic bulk velocity  $\beta < \beta_n = (1 - 1/\Gamma_n^2)^{1/2}$  [19],

$$\beta(R) = \frac{\beta_n}{1 + (\Gamma_n \zeta)^{-1}}, \quad \gamma(R) = \frac{1}{(1 - \beta^2)^{1/2}} = \frac{\Gamma_n \zeta + 1}{(\zeta^2 + 2\Gamma_n \zeta + 1)^{1/2}}, \quad (14)$$

where

$$\zeta(R) = \frac{dM_n}{dm} = \frac{M_n}{R_\beta} \left( \frac{dm}{dR} \right)^{-1}, \quad (15)$$

and  $m(R)$  is ambient mass enclosed by radius  $R$ . There exists a characteristic radius  $R_{\text{trail}}$  where the trail becomes nonrelativistic ( $\beta = 0.5$ ). It is defined by condition  $\zeta = \Gamma_n^{-1}$  [see Eq. (14)], which requires about 10 e-foldings of the decay (for a typical  $m_\beta \sim m_{\text{dec}} \sim 10^{-5} M_n^0$ ). Thus,

$$R_{\text{trail}} \approx 10R_\beta = 0.8 \times 10^{17} \left( \frac{\Gamma_n}{300} \right) \text{ cm}. \quad (16)$$

$R_{\text{trail}}$  depends very weakly (logarithmically) on the ambient density and the initial neutron fraction of the fireball,  $X_n$ .

The decaying N-shell not only accelerates the ambient medium. It also compresses the medium, loads with new particles, and heats to a high temperature. The rest-frame density and relativistic enthalpy of the trail are

$$n = n_0(1 + \zeta) (\zeta^2 + 2\Gamma_n \zeta + 1)^{1/2}, \quad \mu = \frac{(\zeta^2 + 2\Gamma_n \zeta + 1)^{1/2}}{1 + \zeta}, \quad (17)$$

where  $n_0$  is the medium density ahead of the N-shell. For  $\Gamma_n^{-1} < \zeta < \Gamma_n$  one finds  $\mu \gg 1$ , i.e. the thermal energy of the trail far exceeds its rest-mass energy.

The ion fireball follows the neutron front and collects the trail. As a result, (1) the ion Lorentz factor  $\Gamma$  decreases and (2) a shock wave propagates in the trail material. The shock has a Lorentz factor  $\Gamma_{\text{sh}} \gtrsim \Gamma$  and it cannot catch up with the neutron front (unless  $n_0[R]$  falls off steeper than  $R^{-3}$ ). Dynamics and dissipation in the shock are discussed in [19]. We emphasize here that the shock propagates in a relativistically moving, dense, hot, and possibly magnetized medium left behind the leading neutron front. It is very different from the customary shock in a cold and static interstellar medium. A similar situation may take place for fireballs expanding in plerionic surroundings [22].

The neutron impact ceases at  $R_{\text{trail}} \approx 10^{17}$  cm, which can leave an imprint on the observed afterglow. For example, the shock dissipation can have a second bump [19], and a spectral transition is also possible. The arrival time of radiation emitted at  $R_{\text{trail}}$  is approximately  $R_{\text{trail}}/2\Gamma^2c$  (counted from the arrival of first  $\gamma$ -rays). It may be as long as 30 days or as short as a few seconds, depending on the fireball Lorentz factor  $\Gamma(R_{\text{trail}})$ . Recent early observation of a GRB afterglow (GRB 021004) discovered a strong re-brightening at  $10^3$  s, which may be related to neutrons. Also, we do not exclude a possible relevance of neutrons to the 20 day bumps observed in a few GRBs, as the time coincides with  $R_{\text{trail}}/c$ .

Neutron signatures should be absent if the fireball is dominated by a Poynting flux and has extremely low baryon loading. Then the neutron component decouples early, with a modest Lorentz factor  $\Gamma_n$ , and decays at small radii,  $R \ll R_{\text{dec}}$ . The upper bound on  $\Gamma_n$  due to decoupling is  $\Gamma_n \approx 300(\dot{M}_\Omega/10^{26})^{1/3}$  where  $\dot{M}_\Omega$  [g/s] is the mass outflow rate per unit solid angle of the fireball [18].

## 5 Conclusions and prospects

The deceleration radius of GRB fireballs is believed to be in the range  $10^{15} - 10^{17}$  cm, depending on the ambient density and the energy of the explosion. It falls in the interesting range where the prompt  $\gamma$ -rays and free neutrons strongly impact the fireball interaction with the external medium. Therefore, the blast wave, at least at its early stage, should involve the described effects. The upcoming data from *Swift* may be crucial for understanding the basic mechanism of the fireball deceleration. Recent observations of variable early afterglows in GRB 021004 and GRB 030329 indicate that additional complications may be involved such as clumpy ambient medium or refreshed afterglows.

The explosion scenario and its observational signatures depend on the nature of the ejecta. If the fireball is dominated by Poynting flux, the reverse shock emits little energy, and the observed early optical flash must be dominated by the forward shock in the manner described in section 3. If the fireball is dominated by baryons rather than Poynting flux, the reverse shock can also contribute to the flash.

The formation of a leading neutron front appears to be a robust feature of a baryonic fireball, and detection of neutron signatures in the afterglow emission would be important. The current poor understanding of the shock physics and particle acceleration in GRBs impede, however, definite predictions for such signatures, and the model needs to be developed in this direction. For bright bursts,  $E \sim 10^{54}$  erg, the pair-loading radius  $R_{\text{load}}$  of the  $\gamma$ -ray precursor gets comparable to  $R_{\text{trail}}$ , and then the neutrons and  $\gamma$ -rays have a combined impact on the ambient medium. This situation has not been studied yet.

Afterglows observed to date typically have first data points hours or days after

the prompt GRB. The main peak of the blast wave emission is missed. It is expected at seconds or minutes (and possibly overlaps with the prompt  $\gamma$ -rays). The observed tail of the afterglow comes from the slowed-down blast wave, which has an estimated radius  $R \sim 10^{17}$  cm. With *Swift* it may be possible to observe routinely earlier afterglows that come from smaller radii. The afterglow is expected to rise sharply in soft bands at observed time  $t_{\text{obs}} \sim 10E_{53}^{1/2}(\Gamma_{\text{ej}}/100)^{-2}(1+z)$  s. The initial flash must be very soft, and it can emit significant energy before a normal X-ray afterglow sets in, especially in the massive progenitor scenario. The peak of this flash is difficult to detect because it happens quickly, however, future observations may overcome this technical difficulty. *Swift* should be able to see optical emission 30-70 s after the beginning of the burst, and the proposed *ECLAIRs* would detect flashes at much smaller times [11]. A detected initial flash of the afterglow would provide valuable information on the ejecta Lorentz factor, and its time profile and spectrum can give indications on the nature of the ambient medium, and hence the progenitor.

Additional diagnostics for the fireball-medium interaction will be provided by *GLAST*. At the afterglow radii, the ambient medium is likely optically thin (even after  $e^\pm$  loading by the  $\gamma$ -ray precursor), and then the bulk of GRB radiation passes freely through it. However, the most energetic  $\gamma$ -rays may encounter a substantial  $\gamma-\gamma$  opacity made by the scattered radiation. If the ambient medium is a wind from a massive progenitor, the prompt  $\gamma$ -rays should be absorbed above  $\epsilon_{\text{br}} = 5 - 50$  MeV, depending on the density of the wind [5]. This produces a spectral break that should be easily detected by *GLAST*. The scattered  $\gamma$ -rays may also be observed as an echo of the burst [23].

## References

- [1] B. T. Draine, C. F. Mckee, *ARA&A* **31**, 373 (1993)
- [2] P. Madau, C. Thompson, *ApJ* **538**, (2000)
- [3] C. Thompson, P. Madau, *ApJ* **538**, 105 (2000)
- [4] P. Mészáros, E. Ramirez-Ruiz, M. J. Rees, *ApJ* **554**, 660 (2001)
- [5] A. M. Beloborodov, *ApJ* **565**, 808 (2002)
- [6] M. J. Rees, P. Meszaros, *MNRAS* **258**, 41 (1992)
- [7] B. E. Stern, *MNRAS*, submitted, astro-ph/0301384 (2002)
- [8] C. Akerlof et al., *Nature* **398**, 400 (1999)
- [9] P. Mészáros, M. J. Rees, *ApJ* **418**, L59 (1993)

- [10] R. Sari, T. Piran, ApJ **517**, L109 (1999)
- [11] D. Barret et al., astro-ph/0109178 (2001)
- [12] E. V. Derishev, V. V. Kocharovsky, Vl. V. Kocharovsky, A&A **345**, L51 (1999)
- [13] E. V. Derishev, V. V. Kocharovsky, Vl. V. Kocharovsky, ApJ **521**, 640 (1999)
- [14] J. N. Bahcall, P. Mészáros, Phys. Rev. Lett. **85**, 1362 (2000)
- [15] P. Mészáros, M. J. Rees, ApJ **541**, L5 (2000)
- [16] G. M. Fuller, J. Pruet, K. Abazajian, Phys. Rev. Lett. **85**, 2673 (2000)
- [17] J. Pruet, S. E. Woosley, R. D. Hoffman, ApJ **586**, 1254 (2003)
- [18] A. M. Beloborodov, ApJ **588**, 931 (2003)
- [19] A. M. Beloborodov, ApJ **585**, L19 (2003)
- [20] M. Lemoine, A&A **390**, L31 (2002)
- [21] J. Pruet, S. Guiles, G. M. Fuller, ApJ **580**, 368 (2002)
- [22] A. Königl, A. Granot, ApJ **574**, 134 (2002)
- [23] P. Madau, R. D. Blandford, M. J. Rees, ApJ **541**, 712 (2000)